10. A. A. Nepomnyashchii, "Stability of wave regimes in a film adhering to an inclined plane," Izv. Akad. Nauk SSSR, Mekh. Zhidk. Gaza, No. 3 (1974).
11. O. Yu. Tsvelodub, "Stationary traveling waves on a vertical liquid film," Izv. Akad. Nauk SSSR, Mekh. Zhidk. Gaza, No. 4 (1980).
12. Yu. B. Ponomarenko, "One form of stationary motion in hydrodynamics," Prikl. Mat. Mekh., 28, No. 4 (1964).
13. L. D. Landau and E. M. Lifshits, Mechanics of Continuous Media [in Russian], Gostekhteorizdat, Moscow (1954).
14. O. Yu. Tsvelodub, "Stationary traveling waves in a vertical liquid film," in: Wave Processes in Two-Phase Media [in Russian], Izd. Akad. Nauk SSSR, Novosibirsk (1980).

# EXPERIMENTAL STUDY OF BUOYANT VORTEX RINGS

B. I. Zaslavskii and I. M. Sotnikov

UDC 532.517.4

Experimental study of the dynamics and the internal structure of buoyant vortex-thermals was initiated in the 1950s. A review of work done outside the Soviet Union is given in [1]. Problems associated with the motion of thermals are discussed in Soviet publications [2-5]. Experimental data from early as well as those obtained from later studies do not cover many aspects of these phenomena and even contradict each other in some cases. The objective of the present investigations is to study as completely as possible the motion of thermals for various values of initial weight defect. The experimental setup and the test results are described in this paper.

1. The setup is shown in Fig. 1. It consists of: a $1.2\times 1.2\times 5$ m airtight container with transparent side walls; a device (D) for producing thermals; pneumatic and measurement systems. The last mentioned consists of hot-wire anemometers (DISA), movie-(K) and photographic camera, stroboscope, and also an apparatus for visualization of thermals.

The device to produce thermal consists of a nozzle with a funnel shaped tip 4 to blow soap bubble and a trigger to puncture the membrane.

The nozzle is connected by a rubber hose to the smoke generator ($G_d$) and further to the mixer (M) where helium, nitrogen, and oxygen were fed from tanks. The partial pressures of each gas in the mixer were measured with the manometer MVP-2.5 which enabled the determination of density with less than 1% error.

The density was varied in the tests by altering the proportions of helium and nitrogen. Oxygen constituted 2.5% by volume in all the tests. It was supplemented by tobacco smoke which was introduced into the soap bubble for coloring it. A small amount of oxygen ensured low smokiness and, consequently, small relative errors in the final determination of the initial density of the thermal.

The trigger consists of an electromagnet 2, a spoke 3 with a needle at its end.

The film is ruptured when the needle punctures the bubble during its descent which began after the application of the starting voltage to the electromagnet and lasted about 0.02 sec.

Besides the device for producing thermals (setup at the bottom of the container) there is a vertical support 5 to which thin streamlined probes 6 are attached at three levels. The anemometer wires are fixed to the probe tips in such a way that their axes coincide with the central axes of the nozzle and the container. Leads from the hot-wires are brought out from the top of the container and connected to hot-wire anemometers whose signals were recorded with automatic recorder H 338.

Flow visualization of the mixture colored by smoke was made with the help of electronic flash ($F_V$) and optical knife laser beam (L) LG-106M which is propagated in a fan shaped manner with the help of the convex mirror 3. The thermal visualized in such a manner was photographed during its motion by the cameras $F_1$ and

Moscow. Translated from Zhurnal Prikladnoi Mekhaniki i Tekhnicheskoi Fiziki, No. 1, pp. 20-26, January-February, 1983. Original article submitted December 24, 1981.

 0021-8944/83/2401-0016 $07.50 

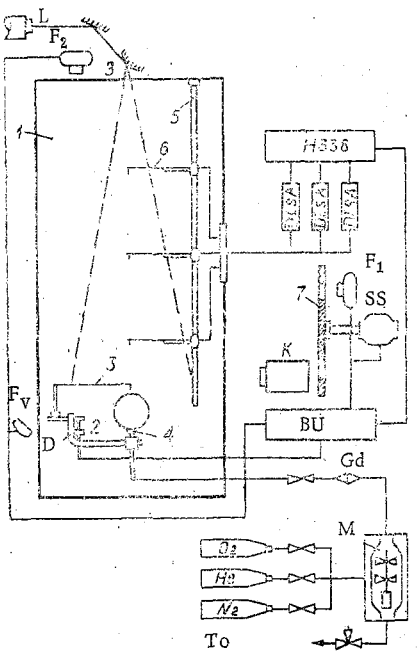

Fig. 1

$F_2$. The latter was controlled by electric pulses. During photography, the stroboscope (SS) consisting of the opaque disk 7 with two slit sectors (~10°), rotates in front of the objective of $F_1$. The disk is setup on the commutator axis of the electric motor which is fed from the variable rectifier.

The stroboscope fulfilled two functions:

1. Light rays passing through the objective of the camera $F_1$ was strobed with a given frequency. Thanks to the strobing, the picture of the moving object was exposed on the film for the entire duration of the process with the shutter open.

2. It actuated the camera $F_2$ and the electronic flash $F_V$ during the interval when the light ray through the objective of $F_1$ is shut off by the disk, making it possible to photograph the object from above without exposing the film in the camera $F_1$.

We note that the thermal sections colored by smoke and falling in the plane of the optical knife were photographed by $F_1$. This strictly vertical plane passes through the hot-wire and the axis of the nozzle 4.

The camera $F_2$ was fixed during the photography at different levels of the contour of the thermal in the horizontal plane. Thus, the spatial distribution of the thermal was actually recorded with the help of $F_1$ and $F_2$ as it rises through a certain interval of time (in our tests, through 0.5-1.0 sec).

Besides the apparatus and devices listed above, the setup includes instruments for the measurement and variation of the frequency of rotation of the stroboscopic disk, generation of trigger pulses for the electronic flash and camera $F_2$, and the timing device for synchronization.

2. We now consider the experimental procedure. The experiment started with the blowing of soap bubble which was gradually filled with the prepared gas mixture colored by smoke and having a given density $\rho_1$. The maximum effective radius $R_0 = \sqrt[3]{3Q_0/4\pi}$ ($Q_0$ is the initial volume of such bubbles) was determined from photographs and the most frequent values of $R_0 \sim 4.5$-5 cm. The bubble collapsed when attempts were made to increase it. The measurement process was started after supplying the trigger voltage to the electromagnet actuating $F_1$ and to the electromagnet 2. The experiments showed that after the supply of the voltage to the latter the bubble collapsed and the gas volume within the bubble completely escaped within 0.04 sec.

The thermal started rising, and at a height $z \sim 1.5R_0$ from the center of the bubble the spherical volume transformed for the first time into a toroid representing the core of the rising vortex ring. Its flow dynamics can be determined by the following functions: $R = R(t)$, $r = r(t)$, $\alpha = dR/dz = \alpha(t)$, $w = w(t)$, $\Gamma(t)$, $\xi(t)$, where r, R are the radii of the toroidal core and its axial circle, $\alpha$ is the aperture angle, w is the ascent rate, $z(t)$ is the coordinate of the center of the core ($z = 0$ is the center of the bubble), $\Gamma(t)$ is the circulation, $\xi = (\rho_0 - \rho_1)/\rho_0$ is the relative drop in density between the core and the external medium.

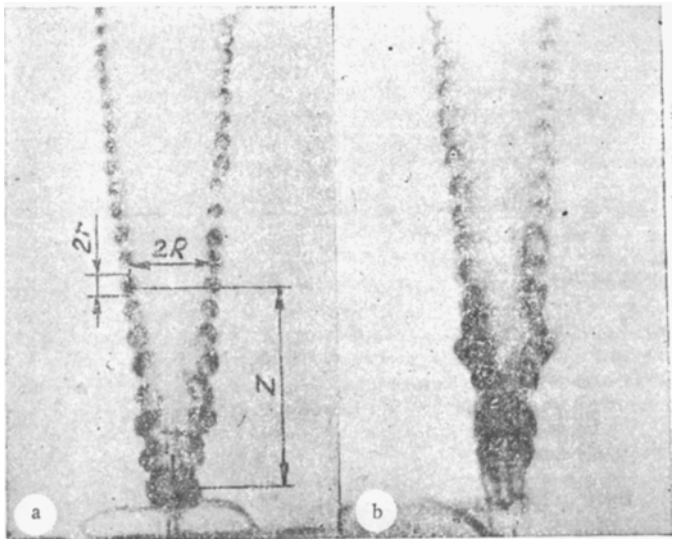


Fig. 2

All these functions can be determined experimentally. In particular, the first four can be determined from the motion pictures filmed with camera $F_1$, provided the center of the thermal does not leave the plane of the optical knife edge. Actually, as mentioned earlier, the camera $F_1$ setup in the stroboscope makes it possible to obtain in one frame, for a given interval, sequential pictures of the axial sections of the core illuminated by the ray from the optical knife edge.

Examples of photographs obtained in such a manner are shown in Fig. 2. Here the moving object was exposed through intervals of 0.1 sec (disk with two apertures, its speed of rotation 5 rps). The determination of r, R, and z are explained in Fig. 2. The parameters $\alpha = dR/dz$ and $w = dz/dt$ can be then determined as $\Delta R/\Delta z$ and $\Delta z/\Delta t$ or by differentiating the functions $R(t)$, $z(t)$. Experiments showed that $\alpha = \alpha_0 = \text{const}$, in the initial segment (up to $z \simeq (10\text{–}15)R_0$), this parameter can be measured directly by goniometer.

A part of the experiments was conducted using a simple procedure with a stationary stroboscopic disk. The ascent of the vortex in this case was photographed simply by an open camera. In this case the individual images of the core sections merge into continuous lines, viz. the traces. Such a procedure gives less information than the stroboscopic pictures but makes it possible to determine in a very simple manner the basic geometric parameters of the core and its trajectory.

If the center of the thermal goes out of the plane of the optical knife edge, the determination of the above functions becomes difficult. It is necessary to make corrections determined by the distance L from the thermal center to the optical knife edge. This distance was measured from photographs obtained with the camera $F_2$ (see Fig. 1). During the experiment $F_2$ operates practically as a motion-picture camera, exposing a number of frames. They make it possible to trace the motion of the thermal projection on the horizontal plane and measure L at any given height. This is necessary not only for the correct determination of the parameters R, $\alpha$, $R_0$ but also for the circulation $\Gamma$.

Hot-wire anemometers were used to determine the latter. Single wire elements were used. The signal from the hot-wire at each level was recorded on one of the three tracks of the automatic recorder, the fourth was used to record the instant camera $F_2$ is triggered. The maximum amplitude of the anemometer signals from the recorder were transformed with the help of calibration curves to the values of $u_i$ (u is the particle velocity in the horizontal plane of symmetry of the thermal, i is the number of the tier). The quantity $\Gamma_i$ was determined from the equation [4]

$$\Gamma_i = -\pi u_i R_i (1 - \delta_i^2)/E(\delta_i). \tag{2.1}$$

Here $\delta_i = l_i/R_i$; $E(\delta_i)$ is the elliptic integral; $l_i$ is the distance from the vortex ring center to the hot-wire at the instant of crossing the corresponding level, i.e., at the moment of measuring $u_i$. In all our experiments $l_i/R_i \ll 1$.

In this case

$$\Gamma_i \approx 2R_i u_i (1 - 0.75\delta_i^2). \tag{2.2}$$

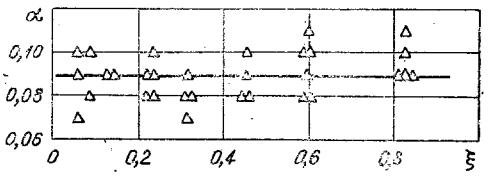


Fig. 3

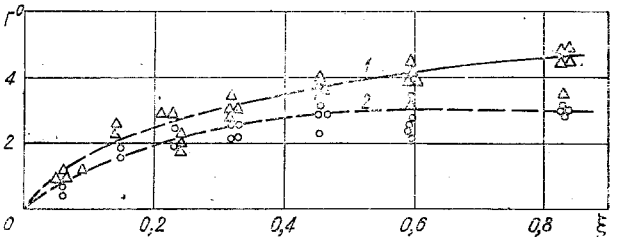


Fig. 4

3. Experimental results are given in Figs. 3-6. Here, and in what follows, the parameter $\Gamma_{i,z}$ are, following [2], replaced by nondimensional parameters $\Gamma_i^0 = \Gamma_i / R_0\sqrt{gR_0}$, $z^0 = z/R_0$.

The values of $\alpha$ for different $\xi$ are given in Fig. 3; the quantities $\Gamma_1^0$, $\Gamma_2^0$ measured at the same values of $\xi$ at the first two levels are given in Figs. 4 (the height of the levels $z_1 = 0.7$m, $z_2 = 1.2$m or $z_1^0 \approx 14$, $z_2^0 \approx 25$, respectively).

These experiments showed that up to a height $z_0 \approx 12$-15, i.e., up to the first level or higher, $\alpha(t) = \alpha$ and $\Gamma(t) = \Gamma$ remain practically constant. The value of these parameters start decreasing when $z^0 > 12$-15. This observation is illustrated by the curves 1 ($\Gamma_1^0(\xi)$) and 2 ($\Gamma_2^0(\xi)$) in Fig. 4. Curve 1 is plotted for experimental data obtained at the first level and 2 for the second level.

The reason for the decrease in circulation can be established on the basis of photographs shown in Fig. 2. The core sections visualized with the optical knife are clearly observed which makes it possible to determine $R(z)$ and $r(z)$ quite accurately and, consequently, also the volume of the toroidal core of the rising vortex $Q(z) = 2\pi^2 r^2 R$ at any level. The value of $Q_0$, as mentioned above, was also obtained from photography. Results of the measurements of the ratios $Q/Q_0$ for two typical cases ($\xi = 0.46$; 0.7, given by points 4 and 3, respectively) are shown in Fig. 5. As seen from these figures, as $z^0 > 15$, the process of the loss of light gas begins, and the circulation also decreases with it. The figure also indicates $t^0 = t\sqrt{g\xi}/\sqrt{R_0}$, obtained from the analysis of photographs as well as from two other experiments ($\xi = 0.32$; 0.83, given by the points 1, 2, respectively).

It has been observed during the studies that for the same initial conditions $R_0$ and $\xi$ there are a series of flow structures inside the thermals. Two extreme variants of this series are easily distinguished. The first one is characterized by a homogeneous core with sharp boundaries (see Fig. 2a), the nature of the motion of such a thermal does not change in the entire observable region of the trajectory ($z \sim 70R_0$). In the case of the second core with blurred boundaries (see Fig. 2b), a spiral structure is observed inside the core, being the probable wake of the rolled up vortex layer formed during the evolution of the thermal.

This structure is less stable and such a thermal breaks down sometimes at a height of $(30\text{-}40)R_0$. The intermediate variants can usually be easily associated with the first or the second type of motion. We observe that when $\xi > 0.4$ the first variant is more frequently observed and when $\xi < 0.4$ (in particular when $\xi < 0.15$) the second type is more frequently observed. Reasons for such nonuniqueness up to the end are not clear. The first type of thermal with homogeneous core (see Fig. 2a), apparently, are similar to migrating turbulent vortex rings [6-8] and the second type is laminar. However, complete analogy is absent since the motion of the thermals in both cases is not identical. Certain small differences in the values of $\Gamma$ and $\alpha$ are observed: in the first case $\Gamma$ is somewhat higher and in the second case $\alpha$ is higher; this variation, apparently, could be associated with the difference in relative time periods $t^0$ and, consequently, relative velocities $w^0 = dz^0/dt^0 = w/\sqrt{g\xi R_0}$, which is seen in Fig. 5. The curve I ($w^0 \approx 0.8$) belongs to sharply observed thermal of the first type and the curve II ($w^0 \approx 1.1$) to the second. However, it is worth observing that at present there is insufficient data for completely establishing such a law.

Finally, a third type of thermal was observed in a number of experiments. They were formed from an initially shapeless mass of light gas with air particles. This mass appeared during the rupture as a result of interaction of two simultaneously appearing thermals.

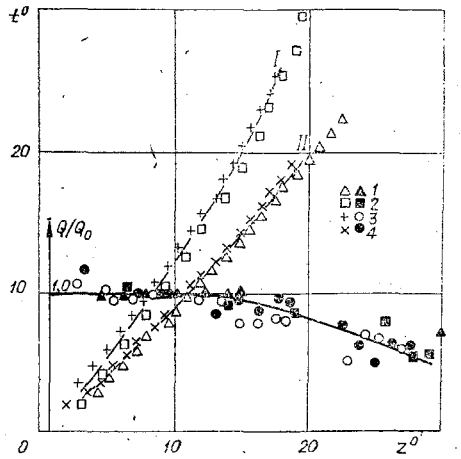


Fig. 5

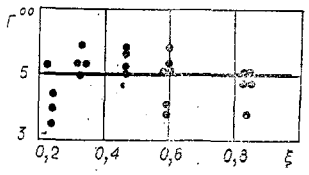


Fig. 6

The formation of the third type of thermal takes place appreciably more slowly. Its parameters are unstable, e.g., values obtained for $\alpha$ varies from 0.2 to 0.4. We note that some values of $\alpha$ are given in [1]. They were obtained from tests conducted with thermals in water, in which water of density greater than that in the container flowed into it from a bucket. Obviously, the discussion in [1] is about thermals of the third type which is laminar, unconcentrated buoyant vortices. They move considerably more slowly and rise through a smaller height than that considered above.

We note that the parameter $\alpha$ of thermals in our experiments was extremely stable: neither the variation in $\xi$ nor artificially introduced disturbance (e.g., puncturing the film from the side or below) appreciably affect $\alpha$ ($\alpha = 0.09 \pm 0.02$, see Fig. 3).

4. Thermals appearing from an initially spherical volume of a gas lighter than the surrounding medium, are transformed into concentrated buoyant vortex ring. In the first segment of the trajectory ($12\text{-}20R_0$) it is possible to consider, with certain approximation, that the only parameter that determines the motion is the weight defect [1] $F = (4/3)\pi R_0^3 g \rho_0 \xi$. Here the explicit dependence of the equation of motion on $\xi$ can be eliminated by switching over to nondimensional parameters and functions $t^{00} = t\sqrt{g\xi}/\sqrt{R_0}$, $z^0 = z/R_0$, $v_1^{00} = v_1/\sqrt{\xi R_0 g}$.

In this case

$$\Gamma^{00} = \Gamma^0/\sqrt{\xi} = \Gamma/R_0\sqrt{\xi R_0 g} = \text{const}, \quad w^{00} = w/\sqrt{\xi R_0 g}.$$

According to our measurements $\Gamma^{00} \approx 5$ (see Fig. 6), $w^0 \simeq 1$. At a height $z^0 > 10\text{-}20$ the effect of exchange processes on the thermal motion becomes appreciable (see Fig. 5) – the motion becomes more complex.

In conclusion, we observe that in the segment $4 < z^0 < 15$ it is possible to obtain a relation between $\alpha$ and $\Gamma$ with the assumption that Biot–Savart law is valid for the buoyant vortex rings. The latter assumption is actually used in deriving the Eq. (2.1). When $r/R \ll 1$, the kinetic energy of such vortex rings with an accuracy to the order $(r/R)^2$ is determined by the equation [9]

$$E_K = (1/2)\Gamma^2 R\rho_0[\ln(8R/r) - 2]. \tag{4.1}$$

Obviously, the flow structure both inside the core and also outside it can be determined with the help of photographs mentioned above. It is quite possible that the true value of r differs from the measured and it is necessary to use a certain effective value $r_e \neq r$ in Eq. (4.1). Assume $r_e = r$. In such a case, differentiating (4.1) with respect to t and with Q = const and equating the result to $d\Pi/dt$, where $\Pi = -\rho_0 \xi Q_0 g z$ is the potential energy, we get

$$\Gamma^0 \simeq 4\sqrt{\pi\xi/3\alpha[2\ln(8R/r) - 1]}. \tag{4.2}$$

$\Gamma^0(\xi)$ computed from Eq. (4.2) is shown by the solid line in Fig. 4, with $\alpha = 0.09$, R and r were obtained from corresponding photographs (of the type shown in Fig. 2a) at the first level.

The authors acknowledge T. N. Anokhina for her help in the work, and S. A. Khristianovich, A. T. Onufriev, and M. D. Shcherbin for the attention given to the work and for useful discussions.

LITERATURE CITED

1. J. S. Turner, Buoyancy Effects in Fluids, Cambridge Univ. Press, England (1973).
2. A. T. Onufriev, "Theory of the motion of a ring under the action of gravity. The rise of the cloud from atomic explosion," Zh. Prikl. Mekh. Tekh. Fiz., No. 2 (1977).
3. V. F. Tarasov, "The motion of the rising vortex ring," in: Dynamics of Continuous Media [in Russian], Vol. 23, Hydrodynamics Institute, Siberian Branch, Academy of Sciences of the USSR, Novosibirsk (1975).
4. V. A. Gorev, P. A. Gusev, and Ya. K. Troshin, "Modeling the rise and combustion of a cloud of light gas in the atmosphere," Dokl. Akad. Nauk SSSR, 205, No. 4 (1972).
5. B. I. Zaslavskii and I. M. Sotnikov, "Motion of vortex rings in homogeneous and stratified media," in: Metrology of Hydrophysical Measurements (Thesis) [in Russian], Moscow (1980).
6. A. A. Lugovtsov, B. A. Lugovtsov, and V. F. Tarasov, "Motion of turbulent vortex ring," in: Dynamics of Continuous Media [in Russian], Vol. 3, Hydrodynamics Institute, Siberian Branch, Academy of Sciences of the USSR, Novosibirsk (1969).
7. A. T. Onufriev and S. A. Khristianovich, "Characteristics of turbulent flow in a vortex ring," Dokl. Akad. Nauk SSSR, 229, No. 5 (1977).
8. V. A. Vladimirov, B. A. Lugovtsov, and V. F. Tarasov, "Suppression of turbulence in concentrated vortex core," Zh. Prikl. Mekh. Tekh. Fiz., No. 5 (1980).
9. S. Patterman, Hydrodynamics of Superfluids [Russian translation], Mir, Moscow (1978).

# SELF-EXCITING POTENTIAL FLUID FLOW, SURROUNDED BY INHOMOGENEITIES, NEAR A CIRCULAR GRID OF PROFILES

E. S. Belyanovskii and V. B. Kurzin

UDC 533.6.011

When a fluid flows through the grid of a turbine machine, in many cases, self-excitation of the velocity field surrounded by inhomogeneities, rotating in the direction of rotation of the grid, occurs. Such phenomena include a rotating discontinuity, which arises in certain regimes in axial turbine machines. In radial grids of centrifugal fans, the rotation of the velocity field was noted and described by Zhukovskii [1]. Recently, a similar phenomenon was also observed while studying fluid flow through a circular grid [2]. The surrounding nonuniformity of the velocity field in [2] was modeled by a displacement of a vortex source from the center of the grid. However, the mechanism for the motion of the vortex source was not examined.

In this paper, the indicated model of fluid flow through a planar circular grid is closed with the help of the equations of motion of the vortex source in the velocity field, perturbed by the profiles of the grid. In addition, the problem of self-excitation of the surrounding nonuniformity is reduced to the problem of the instability of the motion of the vortex source.

1. Experiment. The experiment was performed in a flow channel, consisting of an open tank with diameter 2 m and height 0.8 m (Fig. 1). The tank 1 contained a disk 2 with an aperture at the center, in which a diffuser 3 was inserted. A rod 4, on which a derive shaft 5 is mounted, rotating with the grid 6, was placed on the disk 2. The shaft was rotated by an electrical motor 7 via belt drive 8.

The flow was visualized by introducing confetti into the flow. Figure 2 presents photographs which were made by a camera in a fixed position (Fig. 2a) and rotating synchronously with the grid (Fig. 2b). The photographs clearly show the circular nonuniformity of the velocity field, which is manifested, for example, in the different angles of flow onto the profile. It is noted that this nonuniformity rotates with $\approx 50$ times lower angular velocity than the rotational velocity of the grid.

2. Formulation of the Problem. We shall examine the two-dimensional flow of an ideal incompressible fluid through a circular grid, uniformly rotating with angular velocity $\omega$ (Fig. 3). As is well known, the fluid

Moscow. Novosibirsk. Translated from Zhurnal Prikladnoi Mekhaniki i Tekhnicheskoi Fiziki, No. 1, pp. 26-33, January-February, 1983. Original article submitted January 15, 1982.

0021-8944/83/2401-0021 $07.50  